

USE OF BREAKUP TIME DATA AND VELOCITY HISTORY DATA TO PREDICT THE MAXIMUM SIZE OF STABLE FRAGMENTS FOR ACCELERATION-INDUCED BREAKUP OF A LIQUID DROP

M. PILCH

Sandia National Laboratories, Albuquerque, NM 87185, U.S.A.

C. A. ERDMAN

Nuclear Engineering Department, Texas A&M University, College Station, TX 77843, U.S.A.

(Received 5 January 1987; in revised form 15 July 1987)

Abstract—The mechanisms of acceleration-induced breakup of liquid drops are reviewed briefly. Data on acceleration-induced fragmentation of liquid drops have been collected from the literature and are presented on a consistent basis. Included are critical Weber number data, breakup time data, velocity history data and fragment size data. A triangular relationship based on the concept of a critical Weber number, breakup time data and velocity history data is presented which permits prediction of the maximum size of stable fragments.

1. INTRODUCTION

The work presented here was part of an effort originally initiated to address the question of whether nuclear fuel particles smaller than $1\ \mu\text{m}$ dia could be produced in hypothetical core disruptive accidents (HCDA) in a liquid-metal cooled fast breeder reactor (LMFBR) by the mechanism of hydrodynamic or acceleration-induced fragmentation of larger liquid drops. As the work progressed, the authors became aware of the importance of understanding drop fragmentation in other aspects of reactor safety analysis and, indeed, any transient multiphase flow field involving large ratios of inertial forces to surface tension forces. For example, in an HCDA the dynamics of the disruption are governed by heat, mass and material transport processes; all are dependent on characteristic lengths, e.g. droplet sizes, within the system.

One commonly used technique for dealing with acceleration-induced fragmentation of liquid drops is to assume instantaneous, complete fragmentation to a size determined by a simplistic conventional approach (described later) which may predict particle sizes that are unrealistically small by an order of magnitude or more. Not only are the predicted sizes incorrect, but the assumption of instantaneous fragmentation can dramatically affect the dynamics of the multiphase process. The errors involved in the simple approach to the problem have been quantified, and better methods for correlating breakup times and predicting fragment sizes have been developed in this paper.

The approach suggested here utilizes correlations developed following an exhaustive search of the literature for data on hydrodynamic fragmentation (Pilch 1981). From the collected data, the following key items were obtained: a defensible value for the critical Weber number (minimum ratio of disruptive hydrodynamic forces to stabilizing surface tension forces necessary for acceleration-induced fragmentation); a correlation for the velocity history of accelerated droplets; and a correlation for total breakup time. From the above information, one can accurately predict the maximum size of stable fragments.

The following sections concern themselves with the breakup of isolated liquid drops that are suddenly exposed to a high-velocity flow field that has a density less than that of the drop. In all cases, the flow field is assumed constant on the time scale of drop breakup. The flow field may be a liquid (liquid-liquid system) or a gas (gas-liquid system).

2. DATA COLLECTION FROM THE LITERATURE

Prior to the work reported here and by Pilch (1981) there has been no consistent collection and correlation of experiment data on acceleration-induced fragmentation available to the model developer. Furthermore, there has often been disagreement on the precise meaning of existing data reported in the literature. For example, numerous definitions of drop breakup time have been proposed—due mainly to the difficulty of interpreting experimental observations. Experimental data on breakup time and deformation are commonly obtained from high-speed shadowgraphs of the breakup process. The fragmenting drop is located between a camera and an intense light source; the drop appears as a dark shadow in the photograph (shadowgraph). When the relative velocity between the drop and the flow field is large, mist is generated on the windward surface of the drop and swept into the wake of the drop. The mist completely obscures the drop in shadowgraphs because the mist also appears as a dark shadow. Breakup time and deformation data obtained from shadowgraphs can be misleading because mist makes the drop look much larger than it really is.

In the past, existing data have not been presented in a consistent manner. A variety of independent variables have been used when correlating drop breakup properties (e.g. breakup times). Weber number, Bond number, Reynolds number, free stream velocity, dynamic pressure, shock Mach number and pressure ratio are examples. The Weber number (We) is used as the independent variable throughout this work because it represents the ratio of disruptive hydrodynamic forces to the stabilizing surface tension force:

$$We = \frac{\rho V^2 D}{\sigma}. \quad [1]$$

Here, ρ is the density of the flow field, V is the initial relative velocity between the flow field and the drop, D is the initial diameter of the drop and σ is the surface tension of the drop. Caution is required when reading the literature since some authors define the Weber number in terms of the drop radius instead of the diameter as used here.

Viscous effects on drop breakup are correlated with the Ohnesorge number (On):

$$On = \frac{\mu_d}{(\rho_d D \sigma)^{0.5}}. \quad [2]$$

Here, μ_d is the dynamic viscosity of the drop and ρ_d is the density of the drop. Since the Ohnesorge number involves drop properties only, there is an applied assumption that the viscosity of the continuous fluid is small compared to the viscosity of the drop. The Ohnesorge number is sometimes referred to as the viscosity number, Laplace number or Z number.

A dimensionless time characteristic of drop breakup by Rayleigh–Taylor or Kelvin–Helmholtz instabilities is given by

$$T = t \frac{V \epsilon^{0.5}}{D}. \quad [3]$$

Here t is the dimensional time and ϵ is the flow field/drop density ratio,

$$\epsilon = \frac{\rho}{\rho_d}. \quad [4]$$

2.1. Qualitative Description of Breakup Mechanisms

Previous researchers have often failed to make a careful distinction between the various observed mechanisms of drop breakup. There are five distinct mechanisms of drop breakup as determined by the initial Weber number. These breakup mechanisms, illustrated in figure 1, are:

- | | |
|--|---------------------|
| (1) Vibrational breakup | $We \leq 12$ |
| (2) bag breakup | $12 < We \leq 50$ |
| (3) bag-and-stamen breakup | $50 < We \leq 100$ |
| (4) sheet stripping | $100 < We \leq 350$ |
| (5) wave crest stripping followed
by catastrophic breakup | $We > 350$ |

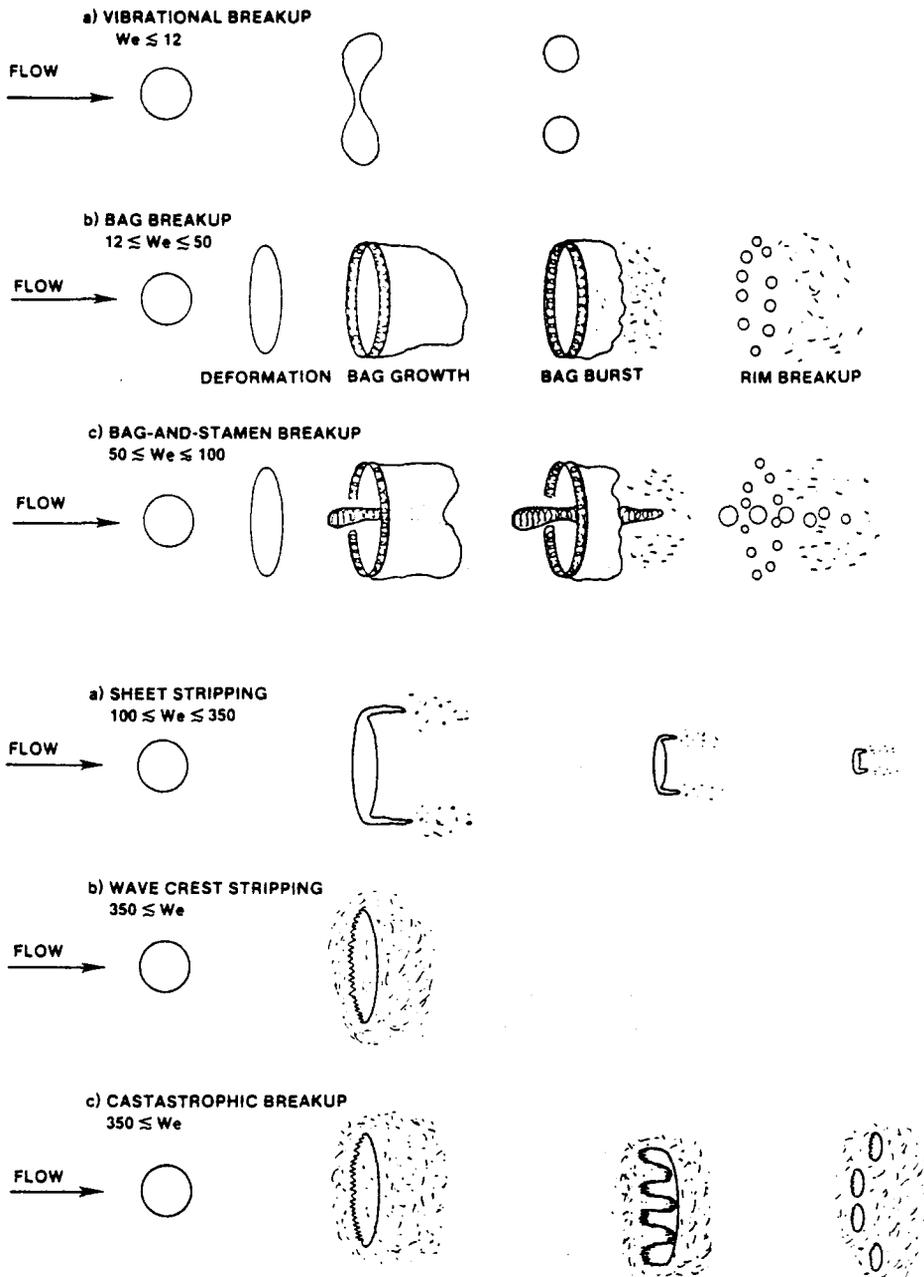


Figure 1. Breakup mechanisms.

“Vibrational breakup” can occur when the Weber number is small; oscillations develop at the natural frequency of the drop. Under certain conditions, the flow field interacts with the drop in such a way as to increase the oscillation amplitude, which in turn causes the drop to decompose into a few large fragments. Vibrational breakup does not necessarily occur in every instance. This breakup mechanism, when it does occur, only produces a few large fragments, and the overall breakup time is long compared to the other breakup mechanisms; consequently, vibrational breakup is not usually considered when drop breakup is studied.

“Bag breakup” is analogous to the bursting of soap bubbles blown from a soap film attached to a ring. A thin hollow bag is blown downstream while it is attached to a more massive toroidal rim. The bag eventually bursts, forming a large number of small fragments; the rim disintegrates a short time later, producing a small number of large fragments.

“Bag-and-stamen breakup” is a transition mechanism that has several features in common with bag breakup. As in bag breakup, a thin bag is blown downstream while being anchored to a massive

toroidal rim; however, a column of liquid (stamen) is formed along the drop axis parallel to the approaching flow. The bag bursts first; rim and stamen disintegration follows. Bag-and-stamen breakup is sometimes referred to as "club breakup", "umbrella breakup" or "claviform breakup".

"Sheet stripping" is distinctly different from the two breakup mechanisms just discussed. No bags are formed; instead, a thin sheet is continuously drawn from the periphery of the deforming drop. The sheet disintegrates a short distance downstream from the drop. A coherent residual drop exists during the entire breakup process.

At still higher Weber numbers, large-amplitude, small-wavelength waves are formed on the windward surface of the drop. The wave crests are continuously eroded by the action of the flow field over the surface of the drop. This process is referred to as "wave crest stripping".

Large-amplitude, long-wavelength waves ultimately penetrate the drop creating several large fragments before wave crest stripping can significantly reduce the drop mass. Drop penetration by large-amplitude surface waves is referred to as "catastrophic breakup". Catastrophic breakup leads to a multistage process in which fragments, and fragments of fragments, are subject to further breakup. This cascading process continues until all the fragments have Weber numbers below a critical value.

This classification of breakup mechanisms is based almost entirely on observations of drop breakup in gas flow fields. Note, however, that similar mechanisms have been reported for liquid-liquid systems. O'Brian (1961) observed bag breakup of an oil drop as it fell under gravity through a second oil. Baines & Buttery (1979) and Theofanous *et al.* (1979) reported similar breakup mechanisms for the breakup of mercury drops in water. More recently, Burger *et al.* (1983) and Kim *et al.* (1983) reported that sheet stripping and wave crest stripping of gallium drops in water occurred over the expected ranges of Weber numbers.

2.2. Critical Weber Number Data

There is a critical Weber number (We_c) below which drop breakup does not occur. The critical Weber number has been investigated experimentally for a variety of fluids which vary widely in surface tension and viscosity. Critical Weber number data from both gas-liquid systems and liquid-liquid systems are shown in figure 2.

The critical Weber number is approx. 12 when the Ohnesorge number is small ($On < 0.1$). Drop breakup at higher Ohnesorge numbers is progressively more difficult and ultimately impossible (in a practical sense). A useful empirical correlation for the critical Weber number by Brodkey (1969) for gas-liquid systems:

$$We_c = 12(1 + 1.077 On^{1.6}). \quad [5]$$

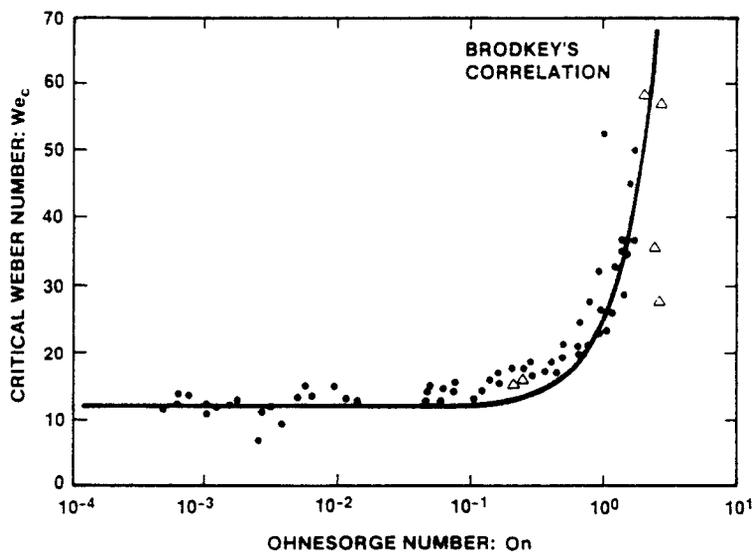


Figure 2. Critical Weber number data: ●, gas-liquid system data from Haas (1964), Hanson & Domich (1956), Hanson *et al.* (1983), Hassler (1970, 1971) and Hinze (1949); △, liquid-liquid system data from Li & Fogler (1978).

A similar expression has been proposed by Gel'fand *et al.* (1975). The data of Li & Fogler (1978) for the breakup of oil drops in water is included in figure 2 supports their conclusion that the critical Weber number for liquid-liquid systems does not differ from that for gas-liquid systems.

2.3. Breakup Time Data

Breakup times are a commonly reported characteristic of drop breakup; however, interpretation of experiment data is difficult as noted above and as evidenced by the many breakup time definitions which appear in the literature. Three characteristic times are of interest: initiation of breakup, primary breakup and total breakup.

Breakup time data for gas-liquid systems are shown in figures 3-5, which will be discussed in greater detail in the following sections. Except for initiation of breakup, all data shown is for low-viscosity ($On < 0.1$) drops. Figure 6 shows some total breakup time data for a liquid-liquid system. Figure 7 summarizes other breakup time data whose definitions are unique.

2.3.1. Initiation of breakup

The definition for initiation of breakup is somewhat arbitrary, and the definition varies according to the breakup mechanism. Start of bag formation marks initiation of breakup for bag breakup and bag-and-stamen breakup. The first sign of a sheet being drawn downstream from the drop marks the initiation of breakup for sheet stripping. The first sign of mist generated on the windward drop surface signals the initiation of breakup for wave crest stripping followed by catastrophic breakup.

The time required to initiate breakup decreases continuously with increasing Weber number for both viscous and nonviscous drops. Wolfe & Anderson (1964) found that large drop viscosity ($On > 0.1$) delayed initiation of breakup without altering the observed breakup mechanism.

A simple empirical correlation is proposed that adequately represents the required time to initiate breakup for viscous and nonviscous drops:

$$T = 1.9(We - 12)^{-0.25} (1 + 2.2 On^{1.6}) \quad [6]$$

The curves from this empirical expression are compared with the data in figure 3. A similar correlation has been proposed by Gel'fand *et al.* (1975).

2.3.2. Primary breakup

Primary breakup time is defined as the time when a coherent residual drop ceases to exist. Primary and total breakup times are equivalent for bag breakup because an intact rim may be

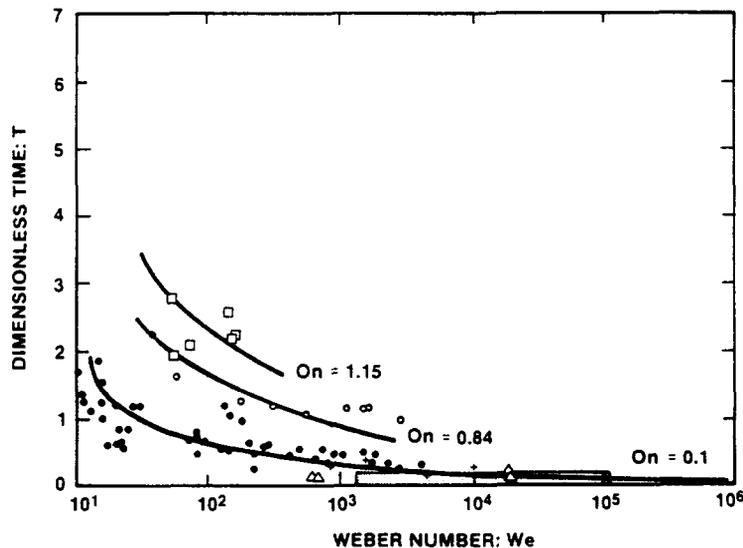


Figure 3. Time to initiate breakup; gas-liquid systems: ●, Wolfe & Anderson (1964); ○, Wolfe & Anderson (1964); □, Wolfe & Anderson (1964); +, Engel (1958); △, Rojec (1963); ■, Krauss (1970).

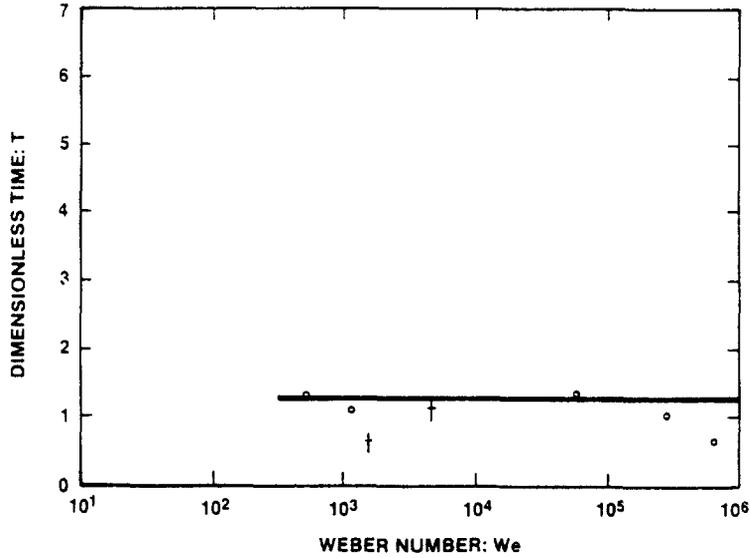


Figure 4. Primary breakup times; gas-liquid systems: \square , Reinecke & Waldman (1970, 1975); $+$, Engel (1958).

viewed as a coherent drop even when the bag has burst. Bag-and-stamen breakup is sometimes followed by bag breakup of a large stamen fragment [Hassler (1970, 1971) and Wolfe & Anderson (1964) contain pictures of this fascinating two-stage process]; however, primary breakup time data is not available. Photographs (Wolfe & Anderson 1964) of sheet stripping indicate that a coherent residual drop exists during the entire breakup process, and there is no evidence of secondary breakup of sheet fragments.

Determination of primary breakup is very difficult when the drop Weber number exceeds about 350 because mist formed by wave crest stripping completely obscures the event. The reader can find a complete discussion of the experimental and analytical evidence for primary breakup in Pilch (1981). The best estimate of primary breakup for this regime is given by

$$T = 1.25, \quad We > 350, \quad [7]$$

as shown in figure 4.

2.3.3. Total breakup

Total breakup time is defined as the time when the drop (if a coherent drop persists) and all its fragments no longer undergo further breakup. Correlations for total breakup time are given by

$$T = 6(We - 12)^{-0.25}, \quad 12 \leq We \leq 18, \quad [8]$$

$$T = 2.45(We - 12)^{0.25}, \quad 18 \leq We \leq 45, \quad [9]$$

$$T = 14.1(We - 12)^{0.25}, \quad 45 \leq We \leq 351, \quad [10]$$

$$T = 0.766(We - 12)^{0.25}, \quad 351 \leq We \leq 2670, \quad [11]$$

and

$$T = 5.5, \quad We \geq 2670, \quad [12]$$

and compared with experimental data in figure 5.

The total breakup times, which are given by the above correlations, are for low-viscosity drops ($On < 0.1$). Based on limited data, Gel'fand *et al.* (1975) proposed a correlation for total breakup time when viscosity is not negligible:

$$T = 4.5(1 + 1.2 On^{1.64}), \quad We < 228. \quad [13]$$

In the inviscid limit, the Gel'fand *et al.* expression is an oversimplification, and clearly [8]–[12] provide a more accurate representation of the existing data.

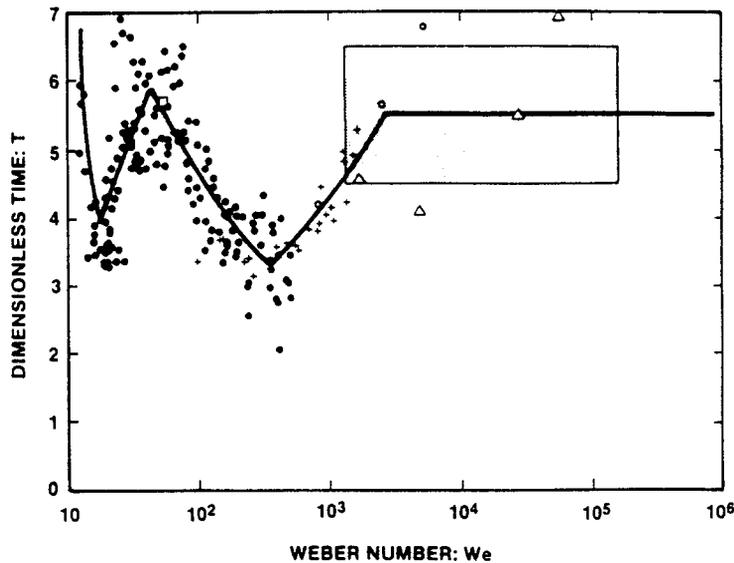


Figure 5. Time for complete breakup, gas-liquid systems: ●, Hassler (1970, 1971); +, Jenkins & Booker (1974); □, Reinecke & Waldman (1975); ○, Engel (1958); △, Ranger (1968); □, Ranger & Nicholls (1969), Krauss (1970) and Mehta (1980);

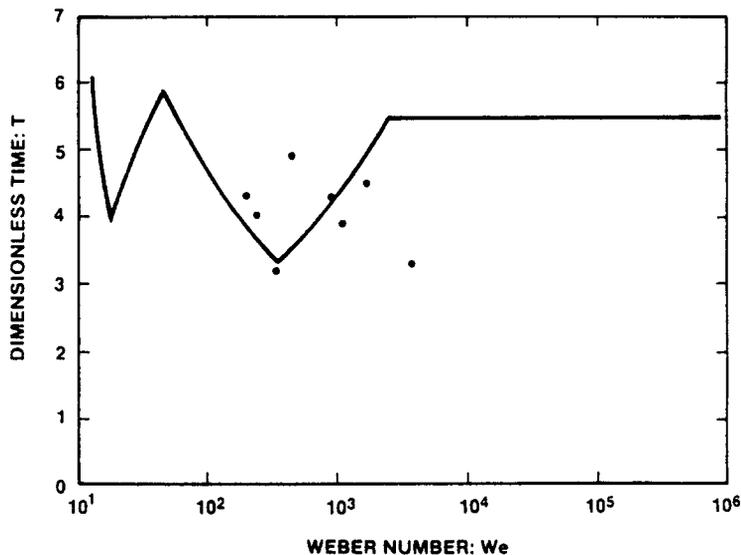


Figure 6. Time for complete breakup; liquid-liquid systems: ●, Baines & Buttery (1979).

The question of breakup times in liquid-liquid systems is an area of ongoing research. The only data to date representing total breakup times is that of Baines & Buttery (1979). Baines & Buttery studied the breakup of mercury drops in water; they reported that the breakup mechanisms were similar to those observed in gas-liquid systems. Baines & Buttery used high-speed motion pictures of the breakup process to determine the breakup time. Breakup time was defined as "... the time at which disintegration of the parent droplet was judged to be essentially complete".

The Baines & Buttery (1979) breakup time data is shown in figure 6 for comparison with gas-liquid system breakup time correlations. There is no discernible trend to the Baines & Buttery data; however, the magnitude of liquid-liquid system breakup times is comparable to total breakup times for gas-liquid systems.

2.3.4. Other breakup time data

This section summarizes data reported as breakup times but where the definition does not clearly fit into the categories defined above. This data is presented in figure 7 where it is compared to the previously recommended correlations.

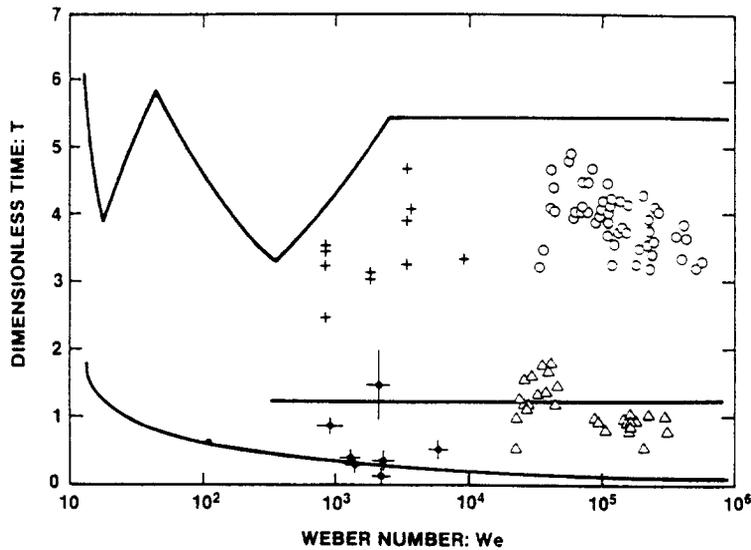


Figure 7. Other breakup time data: Δ , Simpkins & Bales (1972); +, Nicholson (1968); \circ , Kauffman & Nicholls (1971); \bullet , Patel (1978).

Simpkins & Bales (1972) defined breakup as that time when individual waves could be distinguished on the windward surface of the fragmenting drop. This definition is most comparable to primary breakup as defined previously.

Nicholson (1968) calculated the drop velocity by numerically differentiating discrete drop displacement data. He reported that a sharp break in the slope of the velocity curve was observed in each experiment, and he interpreted this behavior as signaling breakup of the drop. Nicholson's data lies somewhat below the total breakup time curve that was presented previously.

Kauffman & Nicholls (1971) defined breakup as the time required for a drop to reach 60% of the free stream velocity, which they noted occurred in about the same time that drops were judged to be completely reduced to a mist. Their data also lies below other definitions for total breakup time. It should be noted, however, that even solid particles will satisfy this definition of breakup.

Patel (1978) and Patel & Theofanous (1980) defined breakup as the time required for the apparent drop diameter to double. Patel's data is comparable to other data for initiation of breakup.

2.3.5. Real times

It is instructive to examine some typical breakup times in real time instead of dimensionless time. Figure 8 shows calculated breakup times for a 1 mm UO_2 drop in sodium or water. Total breakup

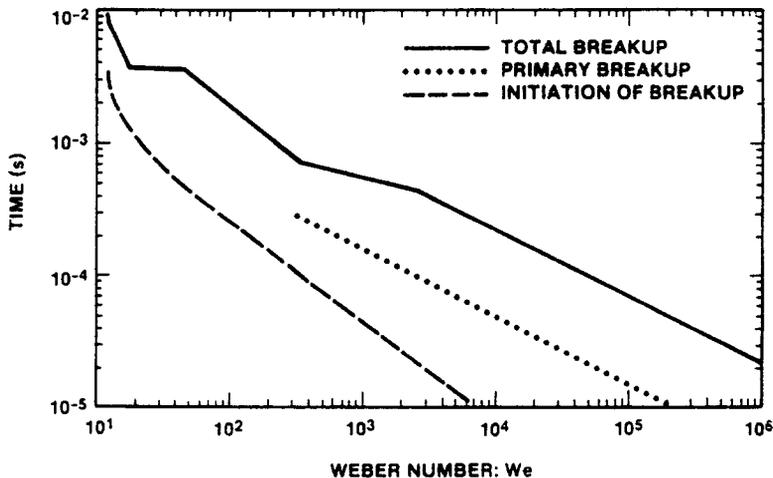


Figure 8. Breakup time for a 1 mm UO_2 drop in sodium or water.

in real time spans three orders of magnitude. The various peaks and valleys seen in the dimensionless breakup time plots appear as slope changes in real time; however, the breakup time decreases continuously with the Weber number in the real time plot.

The breakup process can be quite rapid; nonetheless, a finite time is required for drop breakup. This point is particularly important when incorporating breakup models into computer codes where drop breakup is typically assumed complete during one computational time step. Researchers should be conscious of the fact that drop breakup does not necessarily occur on the time scale of computer time steps, and assuming otherwise may significantly alter their calculated results.

2.4. Drop Displacement, Velocity and Acceleration

Experimenters typically correlate drop displacement with time; drop velocity and acceleration are obtained by differentiating the drop displacement correlation. Interpretation of drop displacement correlations presents difficulties, because drop deformation, mass loss and early breakup influence the acceleration process.

It is important to keep in mind what experimenters actually measure and its relationship to the physics of drop breakup. Researchers measure stagnation point displacement, although center-of-mass displacement is the real quantity of interest. Stagnation point displacement is usually obtained from shadowgraphs; mist may completely obscure the drop, making it impossible to determine the center-of-mass location.

At high Weber numbers, the drop may break up into a number of relatively large fragments which may be subject to further breakup. Shadowgraphs of this dense dispersion give the impression that a coherent drop still exists because mist generated by wave crest stripping masks this early breakup event. Measured drop displacement is in reality the displacement of the slowest moving fragments. The terms drop displacement, drop velocity and drop acceleration are used for the entire breakup process, which may involve several stages of fragment breakup before all fragments are stable.

Although much drop displacement data exists, no model or correlation is currently adequate for all purposes; consequently, the researcher must distinguish between gas-liquid systems and liquid-liquid systems. Furthermore, in the case of gas-liquid systems, the researcher must further distinguish whether the gas flow is compressible with respect to the drop.

2.4.1. Gas-liquid systems

The usual approach to correlating drop displacement does not directly reflect the complicating influence of drop deformation, mass loss and early breakup. The drop is typically modeled as a rigid, constant mass sphere; furthermore, it is customary in the case of gas-liquid systems to neglect the drop velocity (in the lab frame of reference) relative to the free stream velocity. Based on these assumptions, the following expressions for drop displacement (x), velocity (V_d) and acceleration (a) are commonly presented in the literature:

$$\frac{x}{D} = \frac{3}{8} C_d T^2, \quad [14]$$

$$\frac{V_d}{V_\infty^{0.5}} = \frac{3}{4} C_d T \quad [15]$$

and

$$\frac{aD}{V_\infty^2} = \frac{3}{4} C_d. \quad [16]$$

The complicating influences of drop deformation, mass loss and early breakup are reflected in an average drag coefficient (C_d) that is obtained by performing a curve fit to drop displacement data. Table 1 summarizes reported drag coefficients for fragmenting drops. Pilch (1981) recommends that

$$C_d = 2.5 \quad (\text{compressible flow}) \quad [17]$$

and

$$C_d = 1.7 \quad (\text{incompressible flow}) \quad [18]$$

Table 1. Drag coefficients for fragmenting drops: gas-liquid systems

Authors reference	C_d	Weber number range		Reynolds number range		Mach number ^a range	
Aeschliman (1971)	2.30	1.8×10^4	1.1×10^5	4.9×10^4	1.4×10^5	1.4	1.6
Engel (1958)	2.23	4.8×10^3	1.0×10^4	6.3×10^4	9.2×10^4	0.6	0.8
Krauss (1970)	2.73	1.3×10^3	1.2×10^5	1.5×10^4	3.4×10^5	0.7	1.4
Nicholson (1968)	2.67	8.4×10^2	9.2×10^3	6.7×10^3	3.1×10^4	0.8	1.3
Ranger (1968)	2.93	4.8×10^3	1.7×10^5	6.3×10^4	3.0×10^5	0.6	1.5
Reinecke & McKay (1969)	2.13	3.9×10^4	1.7×10^5	2.4×10^4	2.7×10^5	1.4	1.8
Reinecke & Waldman (1975)	2.13	—	1.5×10^3	—	7.1×10^3	—	1.1
Simpkins & Bales (1972)	2.70	—	4.0×10^3	—	1.0×10^4	—	1.7
Jenkins & Booker (1964)	1.89	—	1.1×10^3	—	2.4×10^4	—	0.5
Rabin & Lawhead (1959)	1.7	—	1.2×10^1	1.1×10^3	1.0×10^4	—	0.1
Simpkins (1971)	1.54	5.9×10^1	4.1×10^2	4.3×10^3	1.5×10^4	0.1	0.3

^aRelative to drop.

be used with [15] and [16]. The flow is considered compressible when the Mach number (relative to the drop) exceeds about 0.5. Mehta (1980) and Tempkin & Kim (1980) have shown that the drag coefficient for nonfragmenting drops is also a function of the droplet acceleration. Although this effect is almost certainly important for fragmenting drops, its effect has never been quantified and the effective drag coefficients used here do not explicitly reflect this dependence.

Three problems arise from the use of these correlations: initial drop accelerations are too large; the drop velocity (obtained by differentiating the displacement data) can be too low during the later stages of drop breakup; and the calculated drop velocity can exceed the flow field velocity before breakup is complete.

Modeling drop breakup requires an accurate estimate of the initial drop acceleration. Initially, the drop should accelerate like a rigid sphere because drop deformation and mass loss are insignificant; however, rigid sphere drag coefficients, $C_d = 1$ for compressible flow and $C_d = 0.5$ for incompressible flow, are significantly smaller than data for drop breakup suggest. This is because experimenters measure stagnation point displacement, not center-of-mass displacement, for fragmenting drops. Pilch (1981) has shown that drop deformation alone makes a significant contribution to the observed stagnation point displacement until the actual center of mass is displaced one or two drop diameters.

Kauffman & Nicholls (1971) used streak shadowgraphs to measure directly the time required for a fragmenting drop behind a shock wave ($10^{-2} < \epsilon < 10^{-3}$) to reach 60% of the flow field velocity. Pilch (1981) compared [15] with the Kauffman & Nicholls (1971) data and found poor agreement when $\epsilon < 5 \times 10^{-3}$. Pilch (1981) recommended the following empirical modifications to the drop displacement, velocity and accelerations correlations:

$$\frac{x}{D} = \frac{3}{8} C_d T^2 + BT^3, \quad [19]$$

$$\frac{V_d}{V\epsilon^{0.5}} = \frac{3}{4} C_d T + 3BT^2 \quad [20]$$

and

$$\frac{aD}{V^2\epsilon} = \frac{3}{4} C_d + 6BT. \quad [21]$$

Here, the drag coefficient is set equal to that of a rigid constant-mass sphere, thus providing the correct short-time behavior; the empirical constant (B) is obtained from a curve fit of drop displacement data:

$$C_d = 1, \quad B = 0.116 \quad (\text{compressible flow}) \quad [22]$$

and

$$C_d = 0.5, \quad B = 0.0758 \quad (\text{incompressible flow}). \quad [23]$$

There is no independent streak shadowgraph data like the Kauffman & Nicholls (1971) data against which the modified correlations for incompressible flow can be tested. It is not known which

correlation best represents drop velocity: the conventional correlation or the modified correlation for incompressible flow.

Regardless of which set of correlations is used, one problem still persists: calculated drop velocities at the completion of drop breakup can exceed the flow field velocity for sufficiently large, though physically reasonable and achievable, density ratios (ϵ). This can cause difficulties when calculating fragment sizes by the methods presented later in this paper. It remains a challenge to the researcher to develop drop displacement, velocity and acceleration correlations that have the correct short-time behavior (i.e. accelerate initially like a rigid constant-mass sphere), that have the correct long-time behavior (i.e. drop velocity asymptotically approaches flow field velocity) and that have the correct dependence on density ratio (ϵ). The last point would negate the necessity of having separate sets of correlations for gas-liquid systems and liquid-liquid systems.

In a later section, we will show that the dimensionless breakup time (T) is about 5.5 for a wide range of Weber numbers. As a rule of thumb then, a liquid drop will be displaced 20–40 times its initial diameter during the breakup process.

2.4.2. Liquid-liquid systems

As in gas-liquid systems, the drop is modeled as a rigid constant-mass sphere; however, the drop velocity relative to the flow field velocity is not neglected. The following correlations apply to liquid-liquid systems:

$$\frac{x}{D} = \frac{T}{\epsilon^{0.5}} - \frac{\ln(1 + \frac{3}{4} C_d \epsilon^{0.5} T)}{\frac{3}{4} C_d \epsilon}, \quad [24]$$

$$\frac{V_d}{V \epsilon^{0.5}} = \frac{\frac{3}{4} C_d T}{1 + \frac{3}{4} C_d \epsilon^{0.5} T} \quad [25]$$

and

$$\frac{aD}{V^2 \epsilon} = \frac{3}{4} \left(1 - \frac{\frac{3}{4} C_d \epsilon^{0.5} T}{1 + \frac{3}{4} C_d \epsilon^{0.5} T} \right). \quad [26]$$

These correlations have the advantage that the drop velocity asymptotically approaches the flow field velocity, but they still overpredict the initial drop acceleration because of the large drag coefficients (effective vs rigid constant-mass values for a sphere).

Patel (1978), Patel & Theofanous (1980) and Baines & Buttery (1979) report effective drag coefficients for fragmenting mercury drops that are being accelerated by water:

$$C_d = 2.5 \text{ to } 3.0. \quad [27]$$

Kim *et al.* (1983) correlated the drag coefficient with Reynolds number for fragmenting gallium drops in water:

$$C_d = 5.6, \quad 2 \times 10^4 < \text{Re} < 4 \times 10^4, \quad [28]$$

$$C_d = 3.3, \quad 5 \times 10^4 < \text{Re} < 10^5, \quad [29]$$

and

$$C_d = 1.4, \quad 10^5 < \text{Re} < 2 \times 10^5, \quad [30]$$

where

$$\text{Re} = \frac{\rho V D_0}{\mu} \quad [31]$$

is the Reynolds number and μ is the viscosity of the flow field.

2.5. Fragment Size Data

This section summarizes available fragment size data which is pertinent to the complete breakup of isolated drops. Unfortunately, fragment size information has not been pursued with the same intensity as breakup times. This is the case for gas-liquid systems, while no fragment size data currently exists for liquid-liquid systems.

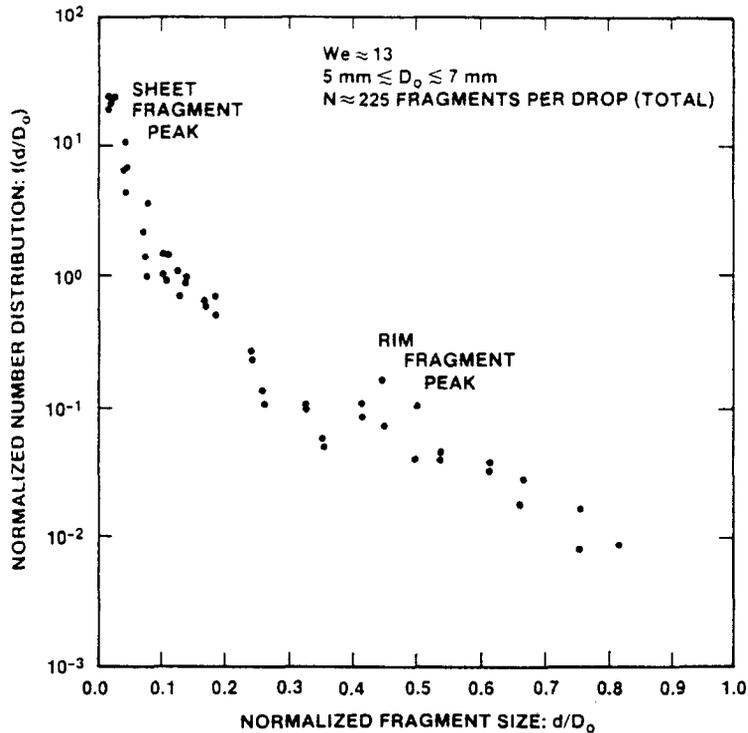


Figure 9. Fragment size distribution for bag breakup: ●, Komabayasi *et al.* (1964).

Ideally, a fragment size *distribution* is most useful to the researcher and, indeed, a few experimentally determined distributions have been reported (i.e. Wolfe & Anderson 1964). These distributions are nearly log-normal (i.e. represented as a straight line on log-probability paper); however, unlike a true log-normal distribution, the experiment distributions clearly indicate an upper limit to fragment sizes. Unfortunately, there is insufficient data on which to characterize fragment size distributions over a broad range of Weber numbers. Consequently, only characteristic or average fragment sizes, which are more commonly reported, are presented here. One exception is the fragment size distribution resulting from bag breakup, which we present here because of its instructive bimodal nature.

2.5.1. Bag breakup distribution

Komabayasi *et al.* (1964) measured the fragment size distribution for water drops undergoing bag breakup near the critical Weber number. Figure 9 shows that the fragment size distribution for bag breakup is bimodal, i.e. it has two peaks. A large number of small fragments are produced when the bag bursts and disintegrates, whereas only a few large fragments are produced when the rim decomposes. Komabayasi *et al.* could not fully define the small fragment peak because of the limitations associated with their collection techniques (fragments $< 100 \mu\text{m}$ could not be identified with certainty).

2.5.2. Characteristic fragment sizes for other breakup mechanisms

Experimental data for three characteristic fragment sizes (maximum, mass median and number median) are presented in figures 10–12. Note that maximum fragment sizes are always about twice as large as mass median fragment sizes, regardless of the Weber number. Weiss & Worsham (1958) also made the same observation for aerosols produced by a wide variety of atomizers. Using this empirical observation, the mass median diameter can be estimated once the maximum fragment size is determined by the techniques discussed later.

3. ESTIMATION OF MAXIMUM STABLE DIAMETER

As indicated earlier, the authors envision the breakup of large accelerating drops ($We > 12$) as a multistage process in which fragments will undergo further breakup as long as the fragment

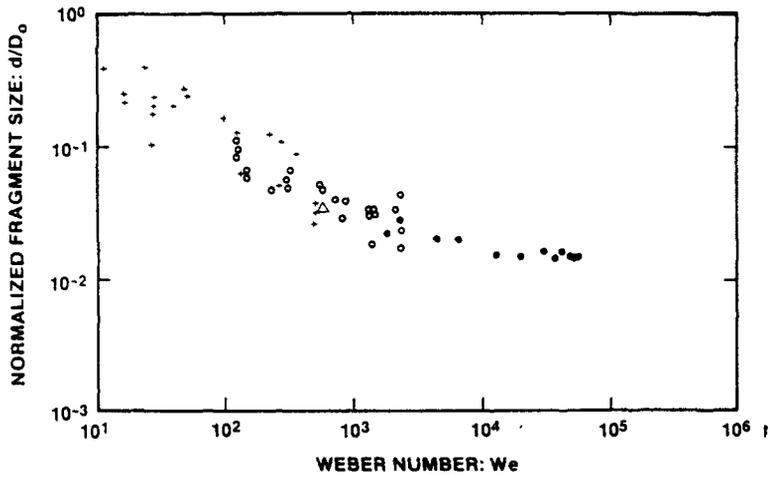


Figure 10. Maximum size of stable fragments; gas-liquid systems: +, Hassler (1970, 1971); O, Wolfe & Anderson (1964); ●, Lane *et al.* (1949), Lane (1951) and Lane & Dorman (1952); Δ, Jenkins & Booker (1964).

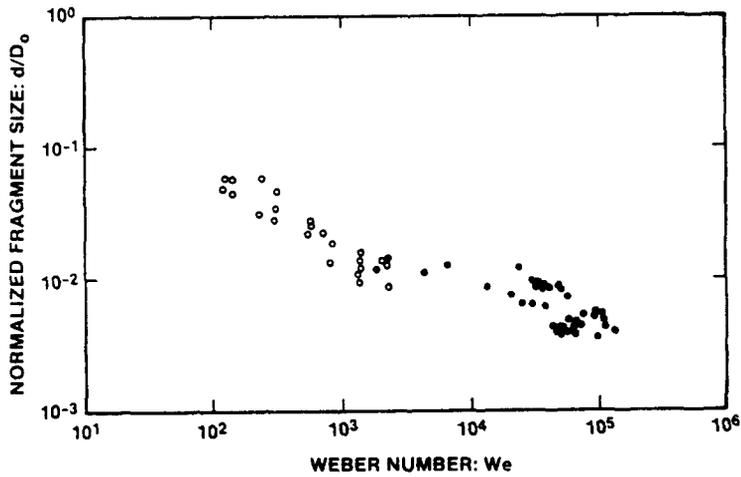


Figure 11. Mass median size of fragments; gas-liquid systems: O, Wolfe & Anderson (1964); ●, Lane *et al.* (1949), Lane (1951) and Lane & Dorman (1952).

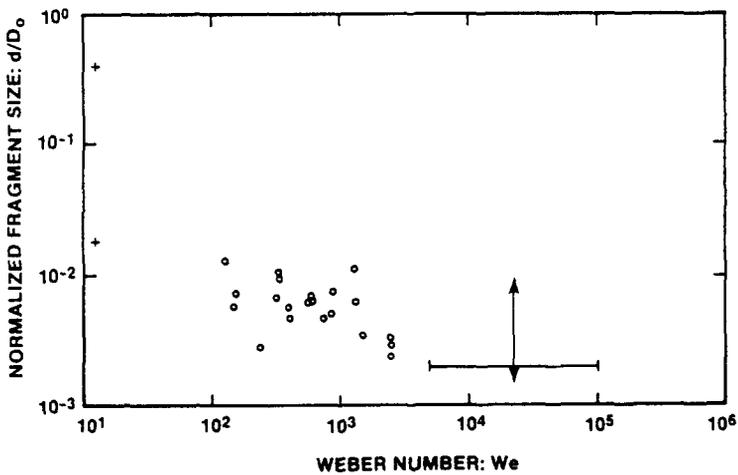


Figure 12. Number median size of fragments; gas-liquid systems; O, Wolfe & Anderson (1964); +, Komabayasi *et al.* (1964); —, Aeschliman (1971); ↔, Ranger (1968) and Ranger & Nicholls (1972).

Weber number exceeds the critical Weber number. When the multistage breakup process is complete, all the fragments will be smaller than a critical size—referred to as the *maximum stable diameter*.

3.1. Conventional Estimate of Maximum Stable Diameter

The conventional estimate of the maximum stable diameter assumes that fragments acquire Weber numbers less than the critical Weber number only because the multistage breakup process produces ever smaller fragments. A fragment whose Weber number equals the critical Weber number has a diameter equal to the maximum stable diameter:

$$d = We_c \frac{\sigma}{\rho V^2}. \quad [32]$$

Here, d is the diameter of the largest stable fragment.

Figure 13 compares experimental data with conventional estimates of the maximum stable diameter. In all cases, the cited authors investigated drop breakup by high-velocity gas fields. Clearly, there is no correlation between the predicted fragment sizes and the experimental data; indeed, predicted fragment sizes can be too small by nearly two orders of magnitude.

3.2. Improved Estimate of the Maximum Stable Diameter

The conventional estimate of the maximum stable diameter fails primarily because of the erroneous assumption that fragment Weber numbers decrease only because fragment sizes decrease. Fragments acquire Weber numbers less than the critical Weber number by two processes: multistage fragment breakup, which produces ever smaller fragment diameters; and fragment acceleration, which decreases the relative velocity between new fragments and the flow field.

An improved estimate of the maximum stable diameter is obtained by accounting for fragment size reduction and decreasing relative velocity:

$$d = We_c \frac{\sigma}{\rho V^2} \left(1 - \frac{V_d}{V}\right)^{-2}. \quad [33]$$

Here, V_d is the velocity of the fragment cloud when all breakup processes cease.

Two additional pieces of information are required to obtain the modified estimate of the maximum stable diameter: a correlation for total breakup time; and a velocity correlation for the accelerating cloud of fragments. These correlations have already been presented in previous sections.

In order to calculate the maximum stable diameter, one proceeds as follows. First, calculate the total breakup time (T) based on the initial Weber number. Use this time in the velocity correlation

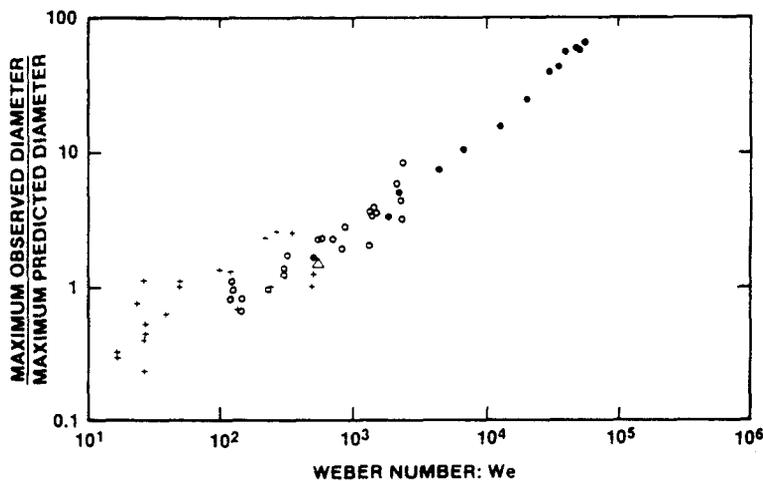


Figure 13. Data comparison with conventional estimates of the maximum stable diameter: +, Hassler (1970, 1971); O, Wolfe & Anderson (1964); ●, Lane (1951) and Lane & Dorman (1952); Δ, Jenkins & Booker (1964).

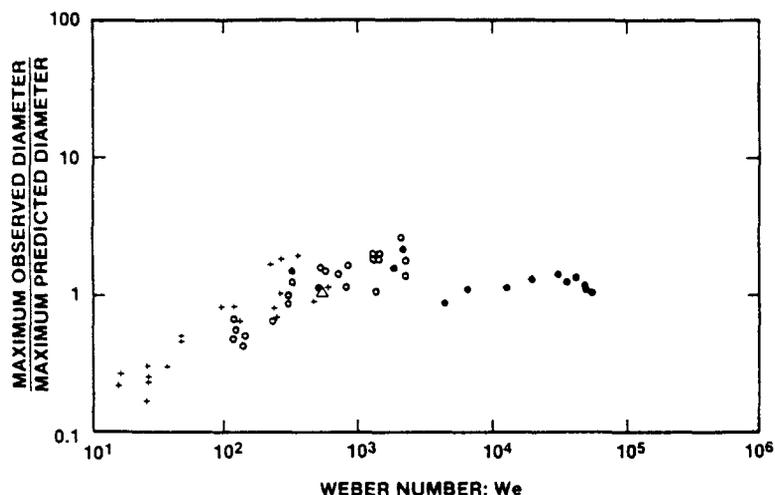


Figure 14. Data comparison with improved estimates of the maximum stable diameter: +, Hassler (1970, 1971); o, Wolfe & Anderson (1964); ●, Lane *et al.* (1949), Lane (1951) and Lane & Dorman (1952); Δ, Jenkins & Booker (1964).

to determine the velocity of the fragmenting drop (V_d) at the time when all fragmentation ceases. Finally, insert V_d into [33] and calculate the maximum stable diameter (d).

Figure 14 compares experimental data with modified estimates of the maximum stable diameter. Note that the ratio of observed predicted fragment sizes is near unity for a wide range of Weber numbers. However, predicted fragment sizes exceed measured fragment sizes when $We \lesssim 350$. This is not a contradiction of the theory; the concept of a maximum stable diameter merely places an upper limit on the largest possible fragment size. The theory does not preclude the possibility that the initial breakup of the parent drop produces primary fragments that are already too small to undergo further breakup. This is consistent with our knowledge of drop breakup mechanisms associated with values of $We < 350$.

Data from Wolfe & Anderson (1964), Lane *et al.* (1949), Lane (1951) and Lane & Dorman (1952) indicate that the mass median size of fragments is one-half the size of the largest stable fragments; their data was obtained from the breakup of isolated parent drops. Weiss & Worsham (1958) studied fragment sizes produced from hydraulic atomizers and pneumatic atomizers. They also observed that the mass median diameter was about one-half the maximum stable diameter. These observations enable us to estimate empirically the mass median diameter once the maximum stable diameter has been calculated by the methods presented above.

Unlike the conventional estimate of the maximum stable diameter, the modified estimate suggests that larger fragments (for a given Weber number) are expected from liquid-liquid systems. This is because drop fragments accelerate more rapidly in the denser flow fields. Experimental data is needed to confirm this prediction.

4. CONCLUSIONS

The concept of a maximum stable diameter suggests a useful method for estimating the size of the largest stable fragments; however, acceleration of the fragment cloud cannot be ignored. The mass median size of fragments can be estimated from the empirical observation that the mass median size is one-half the largest stable size of fragments.

Detailed knowledge about breakup mechanisms is not required when applying the modified concept of a maximum stable diameter as presented here. The concept successfully ties together three separate correlations: critical Weber number correlation; total breakup time correlation; and a velocity correlation for the accelerating cloud of fragments.

By combining the maximum (or mass median) stable diameter results presented here with breakup time correlations, the time-dependent acceleration-induced breakup process can be much more accurately characterized than was possible previously. The implications to safety analysis and to any multiphase transient analysis must be considered.

Acknowledgements—This work was supported by the U.S. Nuclear Regulatory Commission and was performed at the University of Virginia under Contract No. NRC FIN B5616 and at Sandia National Laboratories which is operated for the U.S. Department of Energy under Contract No. DE-AC04-76DP00789.

REFERENCES

- AESCHLIMAN, D. P. 1971 An experimental study of the response of water droplets to flow behind plane shock waves. Report SC-RR-71-0540, Sandia National Labs, Albuquerque, N. M.
- BAINES, M. & BUTTERY, N. E. 1979 Differential velocity fragmentation in liquid-liquid systems. Report RD/B/N4643, Berkeley Nuclear Labs, Berkeley, Calif.
- BRODKEY, R. S. 1969 *The Phenomena of Fluid Motions*. Addison-Wesley, Reading, Mass.
- BURGER, M., SCHWALBE, W., KIM, D. S., UNGER, H., HOHMANN, H. & SCHINS, H. 1983 Two phase description of hydrodynamic fragmentation processes within thermal detonation waves. Presented at the *21st National Heat Transfer Conf.*, Seattle, Wash., Vol. 23.
- ENGEL, O. G. 1958 Fragmentation of waterdrops in the zone behind an air shock. *J. Res. natn. Bur. Stand.* **60**, 245–280.
- GEL'FAND, B. E., GUBIN, S. A., KOGARKO, S. M. & KOMAR, S. P. 1975 Singularities of the breakup of viscous liquid droplets in shock waves. *J. Engng Phys.* **25**, 1140–1142.
- HAAS, F. C. 1964 Stability of droplets suddenly exposed to a high velocity gas stream. *AIChE JI* **10**, 920–924.
- HANSON, A. R. & DOMICH, E. G. 1956 The effect of viscosity on the breakup of droplets by air blasts—a shock tube study. Research Report No. 130, Dept of Aerospace Engineering, Univ. of Minnesota, Minneapolis, Minn.
- HANSON, A. R., DOMICH, E. G. & ADAMS, H. S. 1983 Shock tube investigation of the breakup of drops by air blasts. *Phys. Fluids* **6**, 1070–1080.
- HASSLER, G. 1970 Breakup of large water drops under the influence of aerodynamic forces in a steady stream of stream and stream at subsonic velocities. Presented at the *3rd Int. Conf. on Rain Erosion and Related Phenomena*, Hampshire, England.
- HASSLER, G. 1971 Untersuchungen zur verformung und auflösung von wassertropfen durch aerodynamische krafte im atationaren luft-und qasserstrom bei unterschalgeschwindigkeit. Ph.D. Dissertation, Universitat Karlsruhe, Karlsruhe. Hassler (1970) contains an English translation of much of this material.
- HINZE, J. O. 1949 Critical speeds and sizes of liquid globules. *Appl. scient. Res.* **A1**, 273–288.
- JENKINS, D. C. & BOOKER, J. D. 1964 The time required for high speed airstreams to disintegrate water drops. Report N66-22790, Ministry of Aviation (GB). Aero Research Council Current Papers, CP No. 827, UDC No. 532.6: 533.6.011.
- KAUFFMAN, C. W. & NICHOLLS, J. A. 1971 Shock-wave ignition of liquid fuel drops. *AIAA JI* **9**, 880–855.
- KIM, D. S., BURGER, M., FROHLICH, G. & UNGER, H. 1983 Experimental investigation of hydrodynamic fragmentation of galliumm drops in water flows. Presented at the *Int. Mtg on Light Water Reactor Severe Accident Evaluation*, Cambridge, Mass.
- KOMABAYASI, M., GONDA, T. & ISONO, K. 1964 Life time of water drops before breaking and size distribution of fragment droplets. *J. met. Soc. Japan* **42**, 330–340.
- KRAUSS, W. E. 1970 Water drop deformation and fragmentation due to shock wave impact. Ph.D. Dissertation, Univ. of Florida, Gainesville, Fla.
- LANE, W. R. 1951 Shatter of drops in stream of air. *Ind. Engng Chem.* **43**, 1312–1317.
- LANE, W. R. & DORMAN, R. G. 1952 Further experiments on the shattering of drops by a supersonic air blast. Technical Paper No. 279, Porton, England.
- LANE, W. R., PREWETT, W. C. & EDWARDS, J. 1949 Some experiments on the shatter of drops by transient blasts of air. Technical Paper No. 115, Serial 15, Porton, England.
- LI, M. K. & FOGLER, H. S. 1978 Acoustic emulsification. Part 2. Breakup of the large primary oil droplets in a water medium. *J. Fluid Mech.* **88**, 513–528.
- MEHTA, H. K. 1980 Droplet drag and breakup in shock-wave induced unsteady flows. Ph.D. Dissertation, Rutgers University, New Brunswick, N.J.

- NICHOLSON, J. E. 1968 Drop breakup by airstream impact. Report AD-666-525.
- O'BRIAN, V. 1961 Why raindrops break up—vortex instability. *J. Met.* **18**, 549–552.
- PATEL, P. D. 1978 Hydrodynamic fragmentation of drops. Ph.D. Dissertation, Purdue Univ., West Lafayette, Ind.
- PATEL, P. D. & THEOFANOUS, T. G. 1980 Hydrodynamic fragmentation of drops. *J. Fluid Mech.* **103**, 207–223.
- PILCH, M. 1981 Acceleration induced fragmentation of liquid drops. Ph.D. Dissertation, Univ. of Virginia, Charlottesville, Va.
- RABIN, E. & LAWHEAD, R. 1959 The motion and shattering of burning and nonburning propellant droplets. Report R-1503, Rocketdyne Inc., Canoga Park, Calif. AFOSR TN-59-129.
- RANGER, A. A. 1968 The aerodynamic shattering of liquid drops. Ph.D. Dissertation, Univ. of Michigan, Ann Arbor, Mich.
- RANGER, A. A. & NICHOLLS, J. A. 1969 Aerodynamic shattering of liquid drops. *AIAA Jl* **7**, 285–290.
- RANGER, A. A. & NICHOLLS, J. A. 1972 Atomization of liquid droplets in a convective gas stream. *Int. J. Heat Mass Transfer* **15**, 1203–1211.
- REINECKE, W. G. & MCKAY, W. L. 1969 Experiments on the water drop breakup behind mach 3 to 12 shocks. Report AVATD-0172-69-RR.
- REINECKE, W. G. & WALDMAN, G. D. 1970 An investigation of water drop disintegration in the region behind strong shock waves. Presented at the *3rd Int. Conf. on Rain Erosion and Related Phenomena*, Hampshire, England.
- REINECKE, W. G. & WALDMAN, G. D. 1975 Shock layer shattering of cloud drops in reentry flight. Presented at the *AIAA 13th Aerospace Sciences Mtg*, Pasadena, Calif., AIAA Paper 75-152.
- ROJEC, E. A. 1963 Photographic presentation of shear-type droplet breakup. Report. RR-63-39, Rocketdyne Inc., Canoga Park, Calif.
- SIMPKINS, P. G. 1971 On the distortion and breakup of suddenly accelerated droplets. In *Proc. AIAA/ASME 12th Structures, Structural Dynamics and Materials Conf.*, Anaheim, Calif., AIAA Paper No. 71-325.
- SIMPKINS, P. G. & BALES, E. L. 1972 Water-drop response to sudden accelerations. *J. Fluid Mech.* **55**, 629–639.
- TEMPKIN, S. & KIM, S. S. 1980 Droplet motion induced by weak shock waves. *J. Fluid Mech.* **96**, 135–160.
- THEOFANOUS, T. G., SAITO, M. & EFTHIMIADIS, T. 1979 Fuel coolant interactions and hydrodynamic fragmentation. In *Proc. Int. Mtg on Fast Reactor Safety Technology*, Seattle, Wash., p. 3.
- WEISS, M. A. & WORSHAM, C. H. 1958 Atomization in high velocity air streams. Bumblebee Series, Report No. 277, Esso Research and Engineering Co., Linden, N.J.
- WOLFE, H. E. & ANDERSON, W. H. 1964 Kinetics, mechanism, and resultant droplet sizes of the aerodynamic breakup of liquid drops. AGCD Report No. 0395-04 (18) SP, Aerojet General Corp., Downey, Calif.